

LQ-OCP: Energy-Optimal Control for LQ Problems

Logan E. Beaver, *Member, IEEE*

Abstract—This article presents a method to automatically generate energy-optimal trajectories for systems with linear dynamics, linear constraints, and a quadratic cost functional (LQ systems). First, using recent advancements in optimal control, we derive the optimal motion primitive generator for LQ systems—this yields linear differential equations that describe all dynamical motion primitives that the optimal system follows. We also derive the optimality conditions where the system switches between motion primitives—a system of equations that are bilinear in the unknown junction time. Finally, we demonstrate the performance of our approach on an energy-minimizing submersible robot with state and control constraints. We compare our approach to an energy-optimizing Linear Quadratic Regulator (LQR), where we learn the optimal weights of the LQR cost function to minimize energy consumption while ensuring convergence and constraint satisfaction. Our approach converges to the optimal solution 6,400% faster than the LQR weight optimization, and that our solution is 350% more energy efficient. Finally, we disturb the initial state of the submersible to show that our approach still finds energy-efficient solutions faster than LQR when the unconstrained solution is infeasible.

I. INTRODUCTION

Motion planning is increasingly important with the growth and proliferation of robotics and cyber-physical systems in real-world environments [1]. As these systems reach higher levels of autonomy, it is critical that they react quickly to their environment to guarantee safety and performance [2]. The need for performance must also be balanced with the energy cost of operating these systems. Energy-aware control policies directly reduce the cost to power autonomous systems, and can often be implemented without sacrificing performance [3], [4]. Conserving energy also enables these systems to remain in the field longer [5], and energy-efficient robots can be powered by smaller batteries, which reduces weight, increases efficiency, and decreases price.

Based on our recent results in optimal control [6], in this article we present a new approach to automatically generate optimal trajectories from a specified optimal control problem. In particular, given a system with linear dynamics, linear constraints, and a quadratic cost functional (an LQ system), we derive a linear differential equation that is sufficient and necessary for optimality. This “motion primitive generator” describes every dynamical motion that the system can achieve. This is related to the dynamical motion primitives in the machine learning community [7], however, we can derive closed-form expressions for the dynamical motion primitives analytically because of the LQ structure.

L.E. Beaver is with the Department of Mechanical and Aerospace Engineering, Old Dominion University, Norfolk, VA USA (email: lbeaver@odu.edu).

One common motion planning technique is sample-based approaches, such as A*, RRT* or probabilistic road maps, to build a path that connects the initial and final state together [8]. These approaches tend to yield paths that are not energy efficient, as the path is constructed from a large number of line segments that meet at sharp angles [9]. Furthermore, the path is generally not constructed with a notion of energy-efficiency. This can be somewhat mitigated by using a potential field, control barrier function, model predictive control, or a linear quadratic regulator to drive the system to a reference point in an energy-aware way [8]. These approaches can be used in conjunction with a path, i.e., having the agent track a moving reference, or they can be used to drive the agent to the desired state. However, these approaches tend to focus on *stability* rather than *optimality*, and even if an energy-optimal tracking controller exists, it is only as efficient as the reference trajectory that it is tracking.

One of the most common approaches to optimize LQ problems is the Linear Quadratic Regulator (LQR). LQR approaches drive the system to a reference state, and they have proven to be easy to implement, robust to noise and disturbances, and performant [10]. However, LQR suffers from two major drawbacks: 1) it cannot handle constraints on the state variables, and 2) the cost minimized by LQR controllers is a *weighted tracking error* and has no notion of energy consumption or satisfying boundary conditions. While it is possible to construct an energy-minimizing LQR controller in some cases [11], in general LQR methods cannot be applied to energy-optimal motion planning directly. This is because every component of the state must appear in the LQR objective, whereas the actual energy consumption may be independent of some states, e.g., position. Optimizing for the “wrong” objective function is a major pitfall of optimal control [12], as a solution can be optimal while still having poor performance.

In contrast, we present an approach to generate optimal trajectories for LQ systems that is energy-optimal, obeys state and control constraints, and is guaranteed to satisfy the prescribed (feasible) boundary conditions. In fact, our approach solves a broader class of problems than LQR control—as we allow some states to have 0 cost in the objective function. Intuitively this makes sense; while LQR requires all states to be driven to the reference, we only seek to minimize the variables relevant to energy consumption in our proposed approach.

This work aligns with recent advances in optimal control algorithms. One notable approach is the Method of Evolving Junctions (MEJ) [13], [14], which similarly breaks the optimal control problem down into motion primitives. However,

arXiv:2310.00168v1 [eess.SY] 29 Sep 2023

where MEJ uses a global optimizer to determine the junctions between constraints, we solve the optimality conditions directly. Furthermore, we provide the exact analytic form for all possible motion primitives, whereas MEJ solves for the motion primitives on a case-by-case basis. Similarly, the NOnSmooth Numerical Optimal Control (NOSNOC) package [15] generates optimal solutions for non-smooth systems by exactly resolving the junctions between the different modes of the system. However, where NOSNOC solves the optimal control problem via discretization, we resolve the dynamical motion primitives between junctions exactly. In other words, rather than develop a general-purpose tool to solve a broad range of problems, we present an approach to automatically generate optimal trajectories from the specifications of an LQ problem. We demonstrate this using Matlab's Symbolic Toolbox to construct our cost and constraint matrices, derive the optimal motion primitive generator, and solve for the particular optimal trajectory of our system on the order of seconds. Best of all, the dynamical motion primitives can be computed and stored offline; this enables the optimal trajectory to be computed in real time—even for systems with large numbers of constraints [9].

The remainder of this article is organized as follows: We present the LQ optimal control problem in Section II. We derive the dynamical motion primitives in Section III, and discuss the junctions between primitives in Section IV. Numerical results for a submersible robot in a cave are presented in Section V; finally, we present conclusions and discuss some areas of future work in Section VI.

II. OPTIMAL CONTROL PROBLEM

We consider a linear dynamical system with state $\mathbf{x} \in \mathbb{R}^n$, control action $\mathbf{u} \in \mathbb{R}^m$, and dynamics,

$$\dot{\mathbf{x}} = A\mathbf{x} + B\mathbf{u}, \quad (1)$$

where A, B are appropriately sized matrices. The system is subject to linear constraints, which we denote

$$C\mathbf{x} + D\mathbf{u} \leq \mathbf{e}, \quad (2)$$

where C, D are $c \times n$ and $c \times m$ matrices, \mathbf{e} is an $c \times 1$ vector, and c is the number of constraints. Our objective is to minimize a quadratic function of the state and control variables, i.e.,

$$\begin{aligned} J(\mathbf{x}, \mathbf{u}) &= \mathbf{x}^\top Q\mathbf{x} + \mathbf{u}^\top R\mathbf{u} + 2\mathbf{x}^\top N\mathbf{u}, \\ C(\mathbf{x}, \mathbf{u}) &= \int_0^T J(\mathbf{x}, \mathbf{u}) dt. \end{aligned} \quad (3)$$

Finally, we impose some working assumptions to solve this constrained linear-quadratic optimal control problem.

Assumption 1. The linear system (1) is controllable; the terminal time T is large enough and the constraints (2) admit the existence of a solution.

This article presents a numerical approach to generating optimal control trajectories in real time. Thus, we derive our results under the premise that such a solution exists using Assumption 1. One could relax this assumption by looking

at the reachability of the boundary conditions as in [16], however, this remains an open problem for systems with a large number of constraints.

Assumption 2. The matrix Q in (3) is symmetric.

Assumption 3. The matrix R is full-rank.

Assumption 2 is not fundamental for our analysis, it is only employed to simplify the partial derivatives that arise as part of the optimization. Similarly, Assumption 3 ensures that the control trajectory is smooth and free of discontinuities. Furthermore, both assumptions are straightforward to implement in a real physical system.

To simplify our analysis, we assume that the system dynamics (1) are given in Brunovský normal form [17]. A transformation from a general linear system to Brunovský normal form always exists under Assumption 1. This is a linear change in coordinates to an equivalent system of m integrator chains of length k_i with state \mathbf{s}_i and action a_i , i.e.,

$$\dot{\mathbf{s}}_i = A_i\mathbf{s}_i + B_ia_i, \quad (4)$$

with A_i and B_i matrices of the form,

$$A = \begin{bmatrix} \mathbf{0}_{n_i} & I_{n_i \times n_i} \\ 0 & \mathbf{0}_{n_i}^\top \end{bmatrix}, \quad B = \begin{bmatrix} \mathbf{0}_{n_i} \\ 1 \end{bmatrix}, \quad (5)$$

where $n_i = k_i - 2$, $\mathbf{0}_{n_i}$ is a zero vector of length n_i , and $I_{n_i \times n_i}$ is the $n_i \times n_i$ identity matrix.

With the system in Brunovský normal form, we formulate a linear-quadratic optimal control problem (LQ-OCP).

Problem 1. Generate the trajectory $\mathbf{a}(t)$ that satisfies,

$$\begin{aligned} \min_{\mathbf{a}(t)} & \int_0^T \mathbf{s}^\top Q\mathbf{s} + \mathbf{a}^\top R\mathbf{a} + 2\mathbf{a}^\top N\mathbf{s} \\ \text{subject to:} & (4), \end{aligned} \quad (6)$$

$$\mathbf{g}(\mathbf{s}, \mathbf{a}) = C\mathbf{s} + D\mathbf{a} - \mathbf{e} \leq 0,$$

$$\text{given: } \mathbf{s}(0), \mathbf{s}(T),$$

where T is a fixed time horizon that satisfies Assumption 1 and \mathbf{s}, \mathbf{a} are the stacked vectors of \mathbf{s}_i and a_i , respectively.

Note that the matrices Q, R, N, C, D in Problem 1 are only equal to those in (2) and (3) if the original system is in Brunovský normal form; otherwise, they are computed using the linear coordinate transformation. Furthermore, while we assume the boundary conditions are all known in this work, it is relatively straightforward [6] to generate additional boundary conditions if the initial or final value of a state is left free.

III. DYNAMICAL MOTION PRIMITIVES

To generate a solution to Problem 1 we apply Pontryagin's minimization principle following the standard procedure [16]. We note that this is guaranteed to yield the optimal solution in this case, because Problem 1 is convex with linear constraints [12]. First, to simplify our notation, we define a single vector for each of the $i = 1, 2, \dots, m$ integrator chains,

$$\mathbf{z}_i = \begin{bmatrix} \mathbf{s}_i \\ a_i \end{bmatrix}. \quad (7)$$

For systems with integrator dynamics, i.e., those in Brunovsky normal form, applying Pontryagin's minimization principle yields the ordinary differential equation [6],

$$\sum_{n=0}^{k_i} (-1)^n \frac{d^n}{dt^n} \left(\frac{\partial J}{\partial z_i^n} + \mu^\top \frac{\partial g}{\partial z_i^n} \right) = 0, \quad (8)$$

where z_i^n corresponds to the n th row of the vector z_i , i.e., the n th derivative of the base state z_i^0 . Note that k_i , i.e., the degree of each integrator chain, is the length of the vector z . We can write the optimality condition (8) as a product of vectors, namely, we define

$$\mathbf{D}_i := \left[1, -\frac{d}{dt}, \frac{d^2}{dt^2}, -\frac{d^3}{dt^3}, \dots, (1)^{k_i} \frac{d^{k_i}}{dt^{k_i}} \right]^\top, \quad (9)$$

and let ∇_i denote the gradient operator with respect to z_i . Then, the optimality condition (8) is equivalent to,

$$\left(\nabla_i J + \mu^\top \nabla_i g \right) \mathbf{D}_i = 0. \quad (10)$$

Note that the gradients of the cost and constraints are,

$$\frac{d}{dz} J = 2 \left[\mathbf{s}^\top Q + (N\mathbf{a})^\top, \mathbf{a}^\top R + \mathbf{s}^\top N \right], \quad (11)$$

$$\frac{d}{dz} g = [C, D], \quad (12)$$

To further simplify notation, we combine the constant matrices

$$K = \begin{bmatrix} Q & N \\ N^\top & R \end{bmatrix}, \quad L = [C \quad D]. \quad (13)$$

This implies the derivatives,

$$\frac{\partial}{\partial z} J(z) = 2z^\top K, \quad \frac{\partial}{\partial z} g(z) = L. \quad (14)$$

Finally, we can write (10) for each of the $i = 1, 2, \dots, m$ integrator chains. This yields m ordinary differential equations,

$$\left(2z^\top K_i + \mu^\top L_i \right) \mathbf{D}_i = 0, \quad (15)$$

where K_i, L_i are the rows of (14) corresponding to the states s_i and action a_i . Subsequently, we analyze (15) as a *dynamical motion primitive generator* (e.g., as used in [7]) to exhaustively calculate all possible motion primitives that the optimal trajectory consists of.

When no constraints are active the vector $\mu(t) = \mathbf{0}$ by definition. We re-interpret (15) as the unconstrained dynamical motion primitive,

$$z^\top K_i \mathbf{D}_i = 0, \quad (16)$$

Note that (16) is a homogeneous linear ordinary differential equation of order $2k_i$ with constant coefficients. Differential equations with the form of (16) are straightforward to solve and have a known exponential form. The differential equation (16) is of order $2|s_i|$, thus the coefficients of the unconstrained solution can be solved using the $2|s_i|$ boundary conditions.

In the constrained case, some subset of Lagrange multipliers are non-zero time-varying functions $\mu(t)$. Here, we only consider the elements L that correspond to linearly independent active constraints. Again, this results in a system of linear ordinary differential equations of order $2|s_i|$; the Lagrange multipliers are a system of c constraints can be solved to generate the function $\mu(t)$ in closed form. The result is a system of non-homogeneous linear differential equations with constant coefficients of order $2|s|$,

$$\begin{aligned} 2z^\top K_i \mathbf{D}_i &= -\mu^\top L_i \mathbf{D}_i, \\ Lz - e &\leq 0. \end{aligned} \quad (17)$$

IV. CONSTRAINT JUNCTIONS

With the unconstrained and constrained dynamical motion primitives determined, the final challenge is generating the optimal trajectory that satisfies the boundary conditions and remains feasible. In this section, we assume a sequence of constraint activations is given, and demonstrate how the optimal trajectory is solved. We address some approaches to select the sequence of constraints in following sub-sections.

The solution to Problem 1 is a piecewise collection of the unconstrained (16) and constrained (17) dynamical motion primitives. We denote by t_1 the (unknown) time that the system switches between dynamical motion primitives, and refer to this time and the (unknown) state $s(t_1)$ as a *junction* between the two motion primitives. At each junction, we have two possibilities:

- 1) the constraint(s) becomes active only instantaneously at the junction, or
- 2) the constraint(s) become active at the junction and remain active for some non-zero interval of time.

In the following sub-sections we discuss how to automatically solve the optimality conditions at junctions in order to piece the optimal trajectory together.

A. Tangency Conditions

It is critical to ensure that the system can transition through a junction without requiring an infinite impulse control input. This is achieved through the so-called tangency conditions [16], which ensure the system smoothly transitions between constraints by making the constraint an explicit function of the control input. This is optimal under Assumption 3 [16].

For a linear constraint,

$$g = \mathbf{c}^\top \mathbf{x} + \mathbf{d}^\top \mathbf{u}, \quad (18)$$

where \mathbf{c}^\top and \mathbf{d}^\top are rows of the constraint matrices C and D , we take derivatives until the coefficient of \mathbf{u} is non-zero. Taking a single derivative yields,

$$\frac{d}{dt} g = \mathbf{c}^\top A \mathbf{x} + \mathbf{c}^\top B \mathbf{u}. \quad (19)$$

We repeat this procedure until the product of \mathbf{u} and its coefficient is non-zero, i.e.,

$$\frac{d^q}{dt^q} g = \mathbf{c}^\top A^q \mathbf{x} + \mathbf{c}^\top A^{(q-1)} B \mathbf{u}. \quad (20)$$

Note that under Assumption 1 the matrices A and B are controllable, thus the product $A^{(k)}B$ is guaranteed to have a non-zero product with \mathbf{c}^\top for some $k \in \{0, 1, 2, \dots, n-1\}$. Therefore, the general tangency condition and higher-order constraint with index c is,

$$\mathbf{N}_c = \begin{bmatrix} \mathbf{c}^\top \mathbf{s} - e_c, \\ \mathbf{c}^\top A \mathbf{s}, \\ \vdots \\ \mathbf{c}^\top A^{(q-1)} \mathbf{s}, \end{bmatrix}, \quad (21)$$

$$g_c = \mathbf{c}^\top A^{(q)} \mathbf{s} + \mathbf{c}^\top A^{(q-1)} B \mathbf{a}. \quad (22)$$

where q is the minimum number such that $\mathbf{c}^\top A^{(q-1)} B$ is non-zero.

Finally, we note that if the constraint is only active *instantaneously*, then the tangency conditions may not need to be satisfied—this is because the system immediately exits the constraint and so the constraint $g(\mathbf{s}, \mathbf{a})$ may have a corner. In that case, the above analysis holds except the tangency matrix \mathbf{N}_c only contains the first row.

B. Optimality Conditions

In the unconstrained case, the dynamical motion primitive (16) presents a system of $2|\mathbf{s}|$ order differential equations that describe the optimal motion primitive. There are $2|\mathbf{s}|$ boundary conditions provided in Problem 1, which is sufficient to generate the unconstrained optimal trajectory. If the unconstrained trajectory is infeasible, then the system must switch to a constrained motion primitive somewhere along the trajectory. This can happen in two ways, 1) the system switches to a constrained motion primitive for a finite interval of time, or 2) the system switches to a constrained motion primitive only instantaneously. Furthermore, the system may switch from one constrained motion primitive to another in the same way.

Let t_1 denote the (unknown) time of a junction where the system switches between two dynamical motion primitives. To evaluate a variable v at t_1 we write $v(t_1)$. In general, the control actions and their derivatives may be discontinuous at t_1 ; using the standard notation we write $\mathbf{a}^-, \mathbf{a}^+$ to represent the left and right limits of a variable \mathbf{a} evaluated at t_1 .

In both cases the junction must satisfy a set of optimality conditions with respect to the dual vectors and the Hamiltonian [16], i.e.,

$$\boldsymbol{\lambda}^\top^- = \boldsymbol{\lambda}^\top^+ + \boldsymbol{\pi}^\top \frac{\partial \mathbf{N}}{\partial \mathbf{s}}, \quad (23)$$

$$H^+ = H^- + \boldsymbol{\pi}^\top \frac{\partial \mathbf{N}}{\partial t}, \quad (24)$$

$$\frac{\partial H}{\partial \mathbf{a}^-} = \frac{\partial H}{\partial \mathbf{a}^+} = \mathbf{0}. \quad (25)$$

The time-varying function $\boldsymbol{\lambda}$ is a costate vector, which is the dual variable to the state \mathbf{s} , and the function H is the Hamiltonian, which is analogous to the Lagrangian for dynamical systems. The variable $\boldsymbol{\pi}$ is a constant Lagrange multiplier; the elements of $\boldsymbol{\pi}$ are zero for rows of \mathbf{N} that correspond to inactive constraints, otherwise they are (unknown) scalars that ensure constraint satisfaction at t_1 .

For systems with integrator dynamics, the costates are equal to the partial sums of (15), i.e.,

$$\lambda_i^j = \sum_{n=1}^{k_i=j} (-1)^n \left(\frac{\partial J}{\partial s_i^{j+n}} + \boldsymbol{\mu}^\top \frac{\partial g}{\partial y_i^{j+n}} \right), \quad (26)$$

where λ_i^j is the covector for state s_i^j , i.e., the j^{th} time derivative of base state s_i^0 . Writing (26) as a matrix equation yields,

$$\boldsymbol{\lambda}_i^j = \left(\mathbf{z}^\top K_i + \boldsymbol{\mu}^\top L_i \right) \mathbf{D}_i^j, \quad (27)$$

where \mathbf{D}_i^j is \mathbf{D}_i shifted down $j+1$ rows, and the first j rows are equal to zero. Furthermore, substituting (27) into the jump conditions (23) yields an equation each base state $i = 1, 2, \dots, m$ and each derivative $j = 0, 2, \dots, |\mathbf{s}_i|$,

$$\left((\mathbf{z}^\top^- - \mathbf{z}^\top^+) K_i \right) \mathbf{D}_i^j = \left((\boldsymbol{\mu}^\top^- - \boldsymbol{\mu}^\top^+) L_i \right) \mathbf{D}_i^j + \boldsymbol{\pi} \frac{\partial \mathbf{N}}{\partial s_i^j} \quad (28)$$

Note that, because the state \mathbf{s}_i is continuous under Assumption 3, for each integrator chain i the condition (28) only determines the magnitude that the control action a_i and its derivatives changes at the junction. In particular, setting $j = k_i - 1$ gives a condition on a_i , $j = k_i - 2$ gives a condition on \dot{a}_i and a_i , etc. This yields $|\mathbf{s}|$ equations at the junction.

Next, combining (24) and (25) yields a useful equation [6],

$$\left(J^+ - J^- \right) - \left(\frac{\partial J}{\partial \mathbf{a}} + \boldsymbol{\mu}^\top \frac{\partial g}{\partial \mathbf{a}} \right)^\pm \left(\mathbf{a}^+ - \mathbf{a}^- \right) = \boldsymbol{\pi} \frac{d\mathbf{N}^\mp}{dt}. \quad (29)$$

Substituting in the definitions of \mathbf{g} and J using (2) and (3) yields,

$$\begin{aligned} & (\mathbf{a}^\top R \mathbf{a})^+ + (\mathbf{a}^\top R \mathbf{a})^- - 2\mathbf{a}^{\top+} R \mathbf{a}^- \\ & \pm \boldsymbol{\mu}^{\top\pm} D(\mathbf{a}^+ - \mathbf{a}^-) = \boldsymbol{\pi} \frac{d\mathbf{N}^\mp}{dt}. \end{aligned} \quad (30)$$

This yields one more equation, which determines the unknown junction time t_1 .

C. Summary

In the unconstrained case, the ordinary differential equation (16) implies $2|\mathbf{s}_i|$ unknown constants of integration, which are solved exactly by the $2|\mathbf{s}_i|$ boundary conditions. Because (16) is a linear differential equation, the form of the unconstrained motion primitive can be solved analytically; then the particular trajectory coefficients can be solved online as a linear system of equations evaluated at $t = 0$ and $t = T$.

If the unconstrained case is infeasible, then the system must encounter at least one *junction*. This allows the system to either switch between dynamical motion primitives or to activate a constraint instantaneously. This introduces $2|\mathbf{s}| + c + 1$ unknowns; $2|\mathbf{s}|$ from the dynamical motion primitive (17), c for the time-varying Lagrange multipliers in the constrained motion primitive, and 1 for the unknown time for the junction. The corresponding equations are:

- $|\mathbf{s}|$ equations from continuity in the state,

- $|s|$ equations from the costate jump equations (28),
- c equations from the active constraint $L_c z = e$, and
- 1 equation from the Hamiltonian jump equation (30).

We also note that if a constraint is active only instantaneously, then the tangency matrix has at most one row per constraint. Furthermore, if the system is entering or exiting an unconstrained arc, then the corresponding Lagrange multipliers μ and the tangency vector \mathbf{N} are zeros; this simplifies the optimality conditions significantly.

D. Finding a Constraint Sequence

From the previous sections we can generate the optimal trajectory given the sequence of constraint activations. This is, in general, an open problem. Many contemporary commercial solvers, e.g., NOSNOC [15] and MEJ [13], do not explicitly address how the sequence of constraint activations is generated. Some applications, e.g., minimum-time trajectories in polygonal environments [14], admit a convex decomposition where the search space can be efficiently pruned using branch-and-bound. We have found some success using a minimum distance heuristic to find the a feasible sequence of constraint activations [9], then branch-and-bound can be employed to prune the search space.

Other systems, such as connected and automated vehicles [2], have relatively low dimensionality and few constraints. In this case, it generally efficient to try the unconstrained solution, check what constraint is violated, impose that constraint, and repeat until a solution is found. However, this approach has neither proven to be efficient nor complete in general. Furthermore, the approach scales poorly as the number of vehicles increases to an entire transportation network.

Along with the many pitfalls of applying optimal control in general [12], selecting the optimal sequence of constraint activations is crucial to ensure good performance. This problem is largely unaddressed in the literature, and can reduce an approach from global to local optimality—particularly when many constraints are imposed on the system. This is even true for the convex systems, including the LQ system analyzed in this work.

V. SIMULATION RESULTS

To study the performance of our control algorithm, we consider the problem of a simplified submersible robot navigating through a cave. This is depicted in Fig. 1, where the submersible depicted with the relevant forces and height constraints. The submersible has two control actions, applying forward thrust and changing its buoyancy. The submersible's goal is to reach a goal state while minimizing its energy consumption and avoiding collisions with the floor and ceiling.

Applying Newton's second law yields a simplified submersible model,

$$\begin{aligned} \ddot{x} &= -b_x \dot{x} + u_x, \\ \ddot{y} &= -b_y \dot{y} + B, \end{aligned} \quad (31)$$

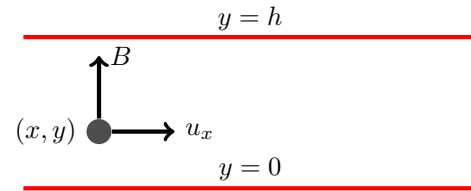


Fig. 1. A submersible robot at point (x, y) with the (net) buoyancy force and forward thrust shown; horizontal lines correspond to the minimum and maximum height.

where b_x and b_y are coefficients of drag, u_x is the forward thrust, and B is the buoyancy, which controlled via,

$$\dot{B} = u_y. \quad (32)$$

We seek to minimize energy consumption of the submersible robot with the objective function,

$$J(\mathbf{x}, \mathbf{u}) = c_1 u_x^2 + c_2 u_y^2 + k_1 \dot{x}^2 + k_2 \dot{y}^2, \quad (33)$$

where the first two terms minimize the actuation effort of thrusting and buoyancy change, and the last two terms penalize the power lost to drag. We constrain the robotic submersible to remain within a minimum and maximum height and subject it to a minimum thrust constraint,

$$0 \leq y \leq h \text{ (cavern height)}, \quad (34)$$

$$u_x \geq T_{\min} \text{ (minimum thrust)}. \quad (35)$$

To put the system in Brunovsky normal form, we perform a linear change of coordinates via feedback linearization,

$$u_x = b_1 \dot{x} + a_x, \quad (36)$$

$$\beta = B - b_2 \dot{y}, \quad (37)$$

$$u_y = a_y + b_2 \beta, \quad (38)$$

where a_x, a_y are the new control actions and β is the net upward acceleration. The result is two integrator chains,

$$\dot{x} = v_x \quad \dot{v}_x = a_x, \quad (39a)$$

$$\dot{y} = v_y \quad \dot{v}_y = \beta \quad \dot{\beta} = a_y. \quad (39b)$$

Under the linear change in coordinates, the objective function (33) becomes $\mathbf{z}^T K \mathbf{z}$, where,

$$K = \begin{bmatrix} 0 & 0 & 0 & 0 & 0 & 0 & 0 & 0 \\ 0 & c_1 b_x^2 + k_1 & 0 & 0 & 0 & 2c_1 b_x & 0 & 0 \\ 0 & 0 & 0 & 0 & 0 & 0 & 0 & 0 \\ 0 & 0 & 0 & k_2 & 0 & 0 & 0 & 0 \\ 0 & 0 & 0 & 0 & c_2 b_y^2 & 0 & 2c_2 b_y & 0 \\ - & - & - & - & - & - & - & - \\ 0 & 2c_1 b_x & 0 & 0 & 0 & c_1 & 0 & 0 \\ 0 & 0 & 0 & 0 & 2c_2 b_y & 0 & c_2 & 0 \end{bmatrix},$$

where

$$\mathbf{z} = [x, v_x, y, v_y, \beta, a_x, a_y]. \quad (40)$$

Furthermore, the constraints in the new coordinate frame are,

$$\mathbf{g} = \begin{bmatrix} 0 & 0 & -1 & 0 & 0 & 0 & 0 & 0 \\ 0 & 0 & 1 & 0 & 0 & 0 & 0 & 0 \\ 0 & -b_x & 0 & 0 & 0 & -1 & 0 & 0 \end{bmatrix} \mathbf{z} - \begin{bmatrix} 0 \\ h \\ -T_{\min} \end{bmatrix} \leq 0.$$

Note that this does not contain an explicit function of the control inputs in rows 1 and 2. Thus, the corresponding tangency conditions N_1 and N_2 are,

$$N_1 = \begin{bmatrix} 0 & 0 & -1 & 0 & 0 \\ 0 & 0 & 0 & -1 & 0 \\ 0 & 0 & 0 & 0 & -1 \end{bmatrix} \mathbf{s},$$

$$N_2 = \begin{bmatrix} 0 & 0 & 1 & 0 & 0 \\ 0 & 0 & 0 & 1 & 0 \\ 0 & 0 & 0 & 0 & 1 \end{bmatrix} \mathbf{s} - \begin{bmatrix} h \\ 0 \\ 0 \end{bmatrix},$$

A. Dynamical Motion Primitives

Recall that we define the state \mathbf{z} as (40). Thus, the submatrices K_1 and L_1 correspond to columns 1, 2, and 6 while K_2 and L_2 correspond to columns 3, 4, 5, and 7 of K and L , respectively. Substituting these values into the optimal motion primitive generator (17) for each integrator chain yields the dynamical motion primitives,

$$-2(c_1 b_x^2 + k_1) a_x + 2c_1 \ddot{a}_x = b_x \dot{\mu}_3 - \ddot{\mu}_3, \quad (41)$$

$$-2k_2 \beta + 2c_2 b_y^2 \ddot{\beta} - 2c_2 \ddot{\beta} \ddot{\beta}_y = \ddot{\mu}_1 - \ddot{\mu}_2. \quad (42)$$

For the constrained case, note that rows 2 and 3 of the constraint matrix correspond to the minimum and maximum channel height, thus for $h > 0$ they cannot be active simultaneously or follow each other in a sequence. This implies that out of the $2^c = 8$ possible dynamic motion primitives, only the following 6 are physically feasible:

- Unconstrained Solution:

$$a_x(t) = c_x e^{\kappa_1 t \pm \kappa_2},$$

$$\beta(t) = c_{y,1} e^{\kappa_3 t \pm \kappa_4} + c_{y,2} e^{\kappa_5 t \pm \kappa_6}. \quad (43)$$

- Minimum Thrust:

$$a_x(t) = c_x e^{-bt},$$

$$\beta(t) = c_{y,1} e^{\kappa_3 t \pm \kappa_4} + c_{y,2} e^{\kappa_5 t \pm \kappa_6}. \quad (44)$$

- Height Constraint (2 cases):

$$a_x(t) = c_x e^{\kappa_1 t \pm \kappa_2}, \quad u_y = 0. \quad (45)$$

- Fully Constrained (2 cases):

$$a_x(t) = c_x e^{-bt}, \quad u_y = 0. \quad (46)$$

Note that $\kappa_1, \kappa_2, \kappa_3, \kappa_4$ are known constants; $c_x, c_{y,i}$ are 2×1 vectors of unknown constants of integration, and c_x is an unknown constant of integration. We emphasize that while (43)–(46) are derived manually here, the dynamical motion primitives can be derived automatically using an automatic differentiation tool; we use the Matlab Symbolic Math Toolbox for this purpose.

For brevity we omit the calculation of the optimal jump conditions (25) and we do not discuss how the sequence of constraint activations is selected. The former can be computed automatically following the previous steps, while the latter is still an open problem in the literature. Instead, we present a simulation results that compares the performance of our proposed approach to an energy-efficient LQR solution.

B. Unconstrained Solution

The parameters used in our simulation study are given in Table I. We selected these parameters to give a relatively high weight to actuation (through c_1 and c_2), while giving a higher penalty to energy lost to forward drag versus vertical drag (via k_1 and k_2). Note that when the submersible starts and ends at rest it stays within $p_y \in [p_y^0, p_y^f]$; similarly, for our travel time of 80s, the travel distance of 100 m is sufficiently large to keep the submersible’s thrust above the minimum value. Thus, the parameters in Table I represent a “nominal” scenario where the submersible follows an unconstrained trajectory.

c_1, c_2	k_1, k_2	b_x, b_y	h	T_{\min}
10	(5, 1)	2.5	25 m	1 N/kg
p_x^0	v_x^0	p_y^0	v_y^0	β^0
0 m	1 m/s	20 m	0 m/s	0 N/kg
p_x^f	v_x^f	p_y^f	v_y^f	β^f
100 m	1 m/s	1 m	0 m/s	0 N/kg

TABLE I

PARAMETERS, INITIAL CONDITIONS, AND FINAL CONDITIONS USED FOR THE SIMULATION STUDY OVER A HORIZON OF $T = 80$ SECONDS.

We present the unconstrained submersible trajectory in Fig. 2. Note that we do not use (43)–(46) in our simulation, rather we include the time for Matlab to generate and solve the differential equations using Matlab’s Symbolic Math Toolbox on a desktop PC (i5 CPU @ 3.2Gz, 16 GB of RAM) using Matlab 2018b. We start by constructing (16) for each integrator chain; this takes approximately 1.3 seconds. Next, we solve the differential equations to generate the optimal motion primitives; this takes 0.375 seconds for the general solution and 1.316 seconds for the particular solution. We take the difference to estimate the time required to apply the boundary conditions as 0.941 seconds. Finally, we convert the particular solution from a symbolic representation into a Matlab function using the `matlabFunction()` command—this takes approximately 11.3 seconds, and it allows us to evaluate the state or control action of the vehicle at any instant of time along the trajectory. Overall, we compute the optimal trajectory from Problem 1 in approximately 14 seconds—and most of the computations can be performed offline.

For the sake of comparison, we also generated a trajectory using an LQR controller [10]. LQR solves an unconstrained optimal control problem with an objective of the form (3). It seeks to do this by finding the optimal feedback matrix K_{lqr} such that the optimal feedback law is,

$$\mathbf{a} = -K_{lqr} \mathbf{s}. \quad (47)$$

The feedback gain K_{lqr} is time-varying for finite-horizon problems, but it can be approximated by the steady-state solution over large time horizons by solving the algebraic Riccati equation [10] that assume steady-state operation. This can be achieved almost instantaneously using the `lqr()` command in Matlab, and is a standard approach in the

literature. However, for energy-aware robotic systems, there are two major caveats that come with LQR control:

- 1) LQR control cannot enforce *constraints*—it only stabilizes the system about a reference.
- 2) LQR does not consider *energy cost*—instead it minimizes a weighted sum of state errors.

To find an energy-efficient LQR solution to the submersible problem, we constructed a new objective function J_{lqr} with the form of (3); this yields 28 optimization variables that correspond to elements of the symmetric matrices Q_{lqr} , R_{lqr} and the full matrix N_{lqr} . To evaluate the performance, we simulated the LQR controller using the parameters in Table I and calculated the energy cost using (3). Finally, we penalized the LQR controller based on its distance from the desired final state, and we applied an infinite penalty if the matrices Q_{lqr} , R_{lqr} , N_{lqr} were infeasible—i.e., did not admit a solution to the Riccati equation or violated the height constraints. Note that we must solve this additional optimization problem because our cost matrix (13) does not admit an LQR solution!

The LQR optimization problem is non-linear, non-smooth, and high-dimensional; thus, we employed a genetic algorithm using Matlab’s Global Optimization Toolbox. We used the default parameters (200 population, 2,800 maximum iterations, 10 elites), and ran the algorithm until it converged after almost 1,000 iterations. This required simulating the LQR system 196,480 times, and 68,958 of these evaluations were infeasible ($\approx 35\%$). The total computational time was 914 seconds, or approximately 15 minutes—this is an order of magnitude larger than the 14 seconds required for our proposed method on the same PC.

A comparison between our proposed approach and the LQR approach is presented in Fig. 2. While both approaches stay within the bounds, the LQR solution initially reaches the ceiling of the domain before diving to the final state. We note that the LQR solution also does not reach the desired final state; this is because there is a tradeoff between quickly converging to the final state versus minimizing energy consumption. Again, this tradeoff explicitly appears in the LQR problem because it has no concept of energy-efficiency or constraints—only convergence. The runtime and computational costs of this analysis are summarized in Table II.

	Proposed	LQR	Improvement
Computational Cost	14.2 seconds	914 seconds	6,337%
Energy Cost	8,439 units	39,041 units	363%

TABLE II

COMPUTATIONAL AND ENERGY COST FOR OUR PROPOSED APPROACH COMPARED TO ENERGY-OPTIMAL LQR.

C. Constrained Solution

The trajectory generated in the previous section remains within the domain $p_y \in [p_y^0, p_y^f]$ for the entire duration. This is because the agent starts and ends at rest in the vertical

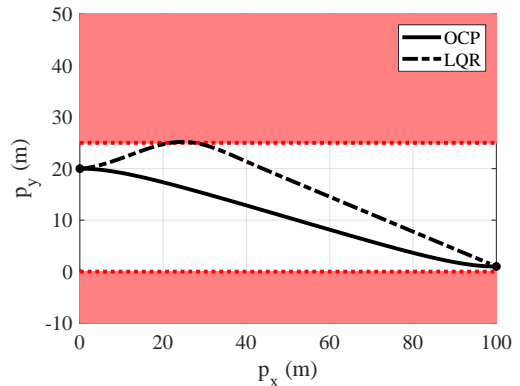


Fig. 2. Resulting submersible trajectories for the unconstrained case.

direction, and overshooting the initial or final state would be energy-inefficient. To force the system to overshoot the bounds of the domain, we adjust the initial velocity and net buoyancy of the submersible to $v_y^0 = -3$ m/s, $\beta^0 = -1N$. This ensures that the unconstrained solution is infeasible, and requires us to follow the motion primitive $p_y = 0$ for some duration of the trajectory. As the final height $p_y^f > 0$, the system will transition from an unconstrained to the height-constrained motion primitive at an unknown time t_1 , then transition back to the unconstrained motion primitive at another unknown time $t_2 \geq t_1$. Note that since the height constraint is independent of the integrator chain $[p_x, v_x, a_x]$, the control input a_x and its derivatives are continuous via (28) and (29); thus the trajectory in the x direction is the unconstrained solution. The unconstrained and constrained solutions are depicted in Fig. 3 and Fig. 4.

If $t_2 = t_1$, then the constraint is only active instantaneously and the system transitions between two unconstrained arcs. In this case the tangency condition is just the constraint $N = [-p_y]$. Note that $v_y \leq 0$ just before the junction, as p_y is decreasing; furthermore, $v_y \geq 0$ just after the junction as $p_y \geq 0$. Thus, it must hold that $v_y(t_1) = 0$. Similarly, as v_y achieves its minimum at t_1 , its derivative $\dot{v}_y = \beta = 0$. Next, note that (28) implies that either a_y is continuous at t_1 or the jump in a_y is equal to the jump in μ_3 . Examining (29) shows that the latter case leads to a contradiction, namely that the Lagrange multiplier $\pi = 0$. Thus, a_y is continuous at t_1 and $\mu(t_i) = \pi \neq 0$. This yields the 7 equations required to generate the optimal trajectory, i.e., continuity in the state, continuity of the control input, and $y(t_1) = v_y(t_1) = \beta(t_1) = 0$. The resulting optimized trajectory is shown in Figs. 3 and 4.

It is critical to realize that including the junction using the constraint $p_y = 0$ produces a *candidate* optimal trajectory. We selected this constraint using a common heuristic, i.e., we imposed the violated constraint as a motion primitive. We could have used the motion primitive corresponding to $p_y = h$ at the junction; this solution is also shown in Fig. 3 and 4. This showcases a major open problem in constrained optimal control: selecting the wrong sequence of constraints can lead

to feasible but sub-optimal solutions. This is particularly true in cases where the cost of an action is linear, e.g., harvesting energy with regenerative braking. Note that even the locally optimal $p_y = h$ solution is still a massive improvement over the LQR solution.

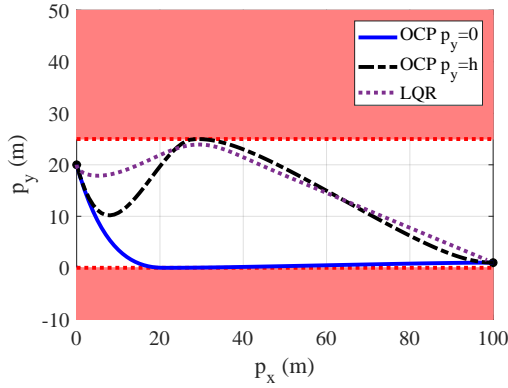


Fig. 3. Resulting trajectories for the constrained case.

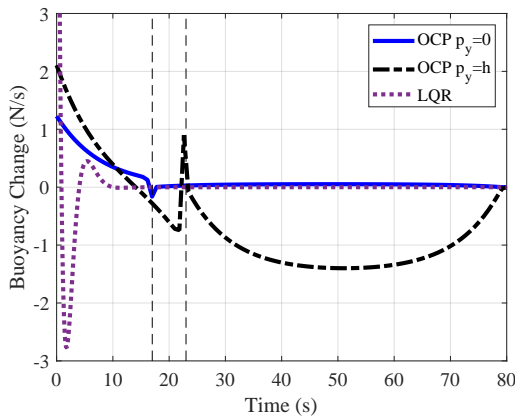


Fig. 4. Change in buoyant force (a_y) for the optimal control and LQR solutions; the left vertical dashed lines demarcates the junction for the $p_y = 0$ case, and the right vertical dashed line demarcates the junction for $p_y = h$.

	Energy Cost	Optimality Gap
OCP with $v_y(t_1) = 0$	8,458 units	0%
OCP with $v_y(t_1) = h$	8,561 units	1.2%
LQR	41,832 units	395%

TABLE III

ENERGY COST FOR PROPOSED AND LQR SOLUTIONS.

VI. CONCLUSIONS AND OUTLOOK

In this article we derived an analytical solution that minimize the energy consumption of controllable LQ systems. We derived the dynamical motion primitive generator (17), and demonstrated how we can activate and deactivate individual constraints to generate all of the system’s dynamical motion primitives offline. We proved that the resulting motion

primitives for an LQ system are linear ordinary differential equations—which always have a closed-form analytic solution. Finally, we compared our proposed approach to an LQR solution and showed a massive improvement both in computational time and system performance.

The results of this article suggest a number of interesting avenues for future work. First, finding optimal solutions to more general problems, e.g., using differential flatness [6], would broadly expand the applicability of these results. Resolving existing computational bottlenecks, including an efficient methods to check for constraint violations and algorithms that yield a feasible sequence of motion primitives, would broadly expand the problems that are amenable to constrained optimal control. Finally, converting multi-agent or game-theoretic problems into strategic-form games is an attractive research direction.

REFERENCES

- [1] H. Christensen, N. Amato, H. Yanco, M. Mataric, H. Choset, A. Drobni, K. Goldberg, J. Grizzle, G. Hager, J. Hollerbach, S. Hutchinson, V. Krovi, D. Lee, W. D. Smart, J. Trinkle, and G. Sukhatme, “A Roadmap for US Robotics – From Internet to Robotics 2020 Edition,” *Foundations and Trends in Robotics*, vol. 8, no. 4, pp. 307–424, 2021.
- [2] B. Chalaki, L. E. Beaver, A. M. I. Mahbub, H. Bang, and A. A. Malikopoulos, “A research and educational robotic testbed for real-time control of emerging mobility systems: From theory to scaled experiments,” *IEEE Control Systems*, vol. 42, no. 6, pp. 20–34, 2022.
- [3] G. Notomista, “Relaxed pfaffian constraints with application to the minimum-energy control of swarms of brushbots,” in *2023 American Control Conference (ACC)*, 2023, pp. 2071–2076.
- [4] L. E. Beaver and A. A. Malikopoulos, “An Overview on Optimal Flocking,” *Annual Reviews in Control*, vol. 51, pp. 88–99, 2021.
- [5] M. Egerstedt, J. N. Pauli, G. Notomista, and S. Hutchinson, “Robot ecology: Constraint-based control design for long duration autonomy,” *Annual Reviews in Control*, vol. 46, pp. 1–7, 1 2018.
- [6] L. E. Beaver and A. A. Malikopoulos, “Optimal Control of Differentially Flat Systems is Surprisingly Easy,” *Automatica (to appear)*, 2023.
- [7] A. J. Ijspeert, J. Nakanishi, H. Hoffmann, P. Pastor, and S. Schaal, “Dynamical movement primitives: Learning attractor models for motor behaviors,” *Neural Computation*, vol. 25, no. 2, pp. 328–373, 2013.
- [8] S. Campbell, N. O’Mahony, A. Carvalho, L. Krpalkova, D. Riordan, and J. Walsh, “Path planning techniques for mobile robots a review,” in *2020 6th International Conference on Mechatronics and Robotics Engineering (ICMRE)*, 2020, pp. 12–16.
- [9] L. E. Beaver, R. Tron, and C. G. Cassandras, “A graph-based approach to generate energy-optimal robot trajectories in polynomial environments,” *IFAC World Congress*, 2023.
- [10] T. Duriez, S. L. Brunton, and B. R. Noack, *Machine learning control-taming nonlinear dynamics and turbulence*. Springer, 2017, vol. 116.
- [11] A. Alavinasab, H. Moharrami, and A. Khajepour, “Active control of structures using energy-based lqr method,” *Computer-Aided Civil and Infrastructure Engineering*, vol. 21, no. 8, pp. 605–611, 2006.
- [12] U. Ledzewicz and H. Schättler, “Pitfalls in applying optimal control to dynamical systems: An overview and editorial perspective,” *Discrete and Continuous Dynamical Systems-B*, vol. 27, no. 11, pp. 6711–6722, 2022.
- [13] W. Li, J. Lu, H. Zhou, and S.-N. Chow, “Method of evolving junctions: A new approach to optimal control with constraints,” *Automatica*, vol. 78, pp. 72–78, 2017.
- [14] H. Zhai, M. Hou, F. Zhang, and H. Zhou, “Method of evolving junction on optimal path planning in flows fields,” *Autonomous Robots*, vol. 46, no. 8, pp. 929–947, 2022.
- [15] A. Nurkanović and M. Diehl, “Nosnoc: A software package for numerical optimal control of nonsmooth systems,” *IEEE Control Systems Letters*, vol. 6, pp. 3110–3115, 2022.
- [16] A. E. Bryson, Jr. and Y.-C. Ho, *Applied Optimal Control: Optimization, Estimation, and Control*. John Wiley and Sons, 1975.
- [17] P. Brunovský, “A classification of linear controllable systems,” *Kybernetika*, vol. 6, no. 3, pp. 173–188, 1970.